JOURNAL OF SOLID STATE CHEMISTRY 85, 220–227 (1990)

Copper-Containing Minerals—I. $Cu_3V_2O_7(OH)_2$, $2H_2O$: The Synthetic Homolog of Volborthite; Crystal Structure Determination from X-Ray and Neutron Data; Structural Correlations

M. A. LAFONTAINE, A. LE BAIL, AND G. FÉREY

Laboratoire des Fluorures, URA CNRS 449, Université du Maine, 72017—Le Mans Cedex, France

Received July 20, 1989; in revised form October 27, 1989

An ab initio structure determination of synthetic volborthite $Cu_3V_2O_7(OH)_2$, $2H_2O$ was performed from X-ray and neutron powder data using a modified Rietveld method. The cell is monoclinic (space group $C2/m$; $Z = 2$) (X rays: $a = 10.606(4)$ Å; $b = 5.874(1)$ Å; $c = 7.213(3)$ Å; $\beta = 94.90(3)°$) (neutrons: $a = 10.607(5)$ Å; $b = 5.864(4)$ Å; $c = 7.214(6)$ Å; $\beta = 94.88(4)°$). The refinement leads to $R_I = 0.035$; $R_P = 0.065$; $R_{WP} = 0.063$ (X rays); and $R_I = 0.060$; $R_P = 0.093$; $R_{WP} = 0.085$ (neutrons). The structure is built up from defect brucite-type layers in the (001) plane, connected one to each other by pyrovanadate groups. The corresponding pillared and layered framework embeds water molecules. The hydrogen bonding subnetwork is described. Structural correlations are given.

Introduction

In the context of a general study of the physical properties of copper-containing natural minerals, we reproduced the synthesis of volborthite $Cu_3V_2O_8$, $3H_2O$. This compound was known since the 18th century. Later, the physical, chemical, and optical properties were studied by Guillemin (*1*). Leonardsen and Petersen (*2*) assigned it a monoclinic symmetry. However, no structural determination had been carried out so far. Therefore, this paper is devoted to the crystal structure of synthetic volborthite and its structural relationships with some layered and pillared structures. It will show that volborthite is correctly written with the formula $Cu_3V_2O_7(OH)_2$, $2H_2O$.

Experimental

Volborthite was prepared according to the method of Strupler (*3*) from stoichiometric amounts of $CuSO_4$ and V_2O_5 solutions in NaOH medium at 40°C. The partially deuterated sample used for neutron diffraction was prepared in the same way. The compound is poorly crystallized and exhibits broad diffraction lines.

The X-ray powder pattern recorded on a Siemens D501 diffractometer (diffracted beam monochromator; Cu$K\alpha$; 2θ range: 5–120°) agrees with the data of Leonardsen and Petersen (*2*). In order to avoid orientation effects, the X-ray samples were prepared according to the method described in Ref. (*4*). The neutron diffraction pattern of the deuterated sample was recorded on the

0022-4596/90 $3.00

TABLE I

DETAILS OF RIETVELD REFINEMENTS (X RAY AND NEUTRON)

	X ray	Neutron
Lattice constants		
a(Å)	10.606(4)	10.607(5)
b(Å)	5.874(1)	5.864(4)
c(Å)	7.213(3)	7.214(6)
β(°)	94.90(3)	94.88(4)
Volume (Å^3)	447.5(1.8)	447.2(2.1)
Density (g · cm^{-3}):	3.52	3.52
2θ-step scan increment (°)	0.04	0.20
2θ-range (°)	15–115	15–130
λ (Å)	1.54056	2.52370
Number of reflections	340	102
Zero point (2θ)	0.024(4)	−0.376(13)
Reliability factors		
R_I	0.035	0.060
R_P	0.065	0.093
R_{WP}	0.063	0.085
R_E	0.040	0.025
Space group	$C2/m$	$C2/m$

D1B diffractometer (2θ range: 10–130°; λ = 2.5237 Å) at Institut Laue-Langevin in Grenoble.

Data Analysis

The conditions limiting possible reflections (hkl: $h + k = 2n$) lead to the space groups $C2/m$, Cm, or $C2$. The lattice parameters refined from X-ray data are a = 10.606(4) Å; b = 5.874(1) Å; c = 7.213(3) Å; β = 94.90(3)°; v = 447.5 Å^3; and the calculated density is d = 3.52 g/cm^3 for Z = 2.

Individual intensities were extracted from the X-ray powder pattern by a profile fitting procedure which does not need any structural model but constrains the angular position of the reflections to be consistent with the cell parameters (*5*). Table I summarizes the details of data collection.

Intensities were converted into structure factors and used as input data for the program SHELX76 (*6*). Cu^{2+} and V^{5+} were localized by using the direct methods (option TANG of SHELX) and a Fourier synthesis. Scattering factors for Cu^{2+} and V^{5+} were taken from International Tables for X-ray Crystallography (*7*) and O^{2-} from (*8*).

A profile Rietveld refinement using this set of atomic positions as structural model, followed by Fourier difference synthesis, yielded the positions of the remaining oxygen atoms. Reflection (001), very asymetrical, was excluded. This leads to the reliability factors R_I = 0.041; R_P = 0.074; R_{WP} = 0.073.

Refinements performed in the space groups Cm and $C2$ do not improve these results.

At this stage, indications of anisotropic X-ray line broadening were noticed. Such an effect and the anomalously high linewidth of all reflections are not unexpected since the method of synthesis (precipitation) is not favorable to the growth of crystals larger than 1000 Å. So the X-ray data were reexamined using the "size-strain analysis" options of our modified Rietveld method [(*9*) and references therein]. The instrumental profile g was determined from a well-crystallized NiF_2 sample measured under the same conditions; the experimental profile h of $Cu_3V_2O_7(OH)_2$, $2H_2O$ is then reproduced as the convolution product $h = f * g$ (where f is the "true sample" profile)

TABLE II

MEAN SIZE $\overline{M}$ (Å) AND STRAIN VALUES IN SOME CHARACTERISTIC DIRECTIONS

	Directions perpendicular to planes (hkl)					
	$h00$	$0k0$	$00l$	101	110	011
$\overline{M}$ (Å)[a]	216	402	159	154	320	226
$\langle Z_1'^2\rangle \cdot \langle d'^2\rangle \cdot 10^3$ (Å^2)[b]	0.33	1.65	0.38	0.25	0.64	0.58

[a] $\overline{M}$ is related to the "surface" distribution while another definition $\overline{M}1$ exists for a "volume" distribution (obtained from integral breadth for instance). When the size effect is fixed as a Cauchy-like broadening, the relation $\overline{M}1 \approx 2\overline{M}$ is valid.

[b] $\langle Z_n'^2\rangle$ is obtained from $\langle Z_1'^2\rangle$ by the relation $\langle Z_n'^2\rangle = |n|^K \langle Z_1'^2\rangle$, where $\langle Z_1'^2\rangle$ and K are refinable parameters (K = 1.7(1)); $\langle d'\rangle$ = 13.8 Å, see Ref. (*9*).

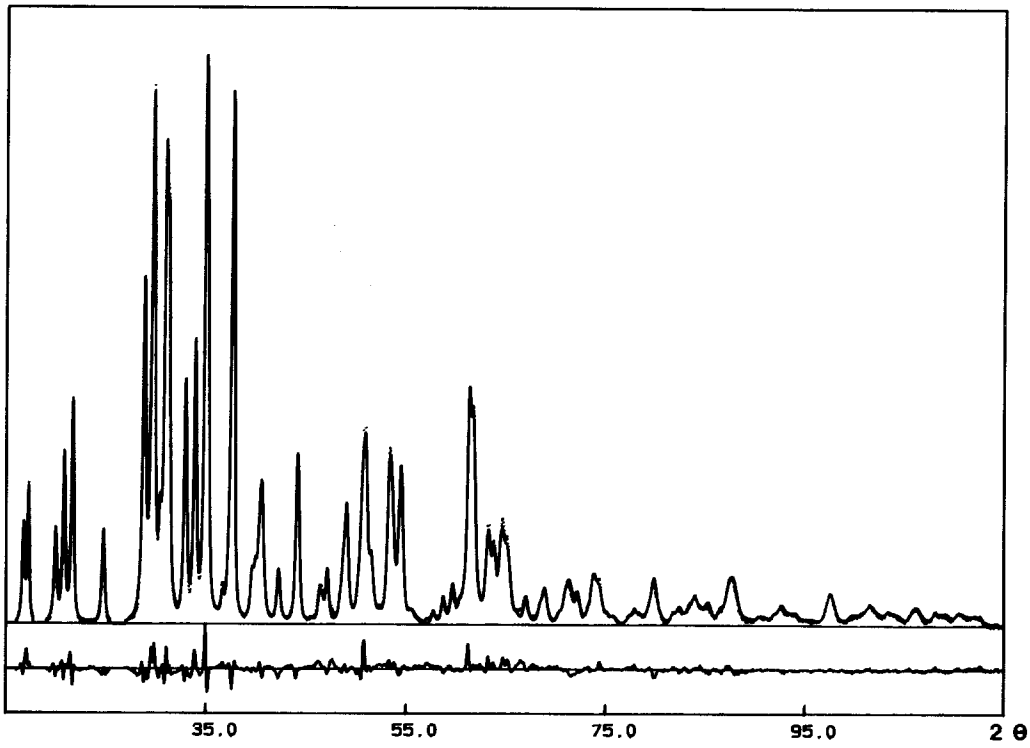

FIG. 1. Observed (...) and calculated (—) X-ray powder patterns. The difference appears below at the same scale.

by means of Fourier coefficients. Assuming a given size distribution (Cauchy), an adjustable strain variation in space, and using an ellipsoid in order to approximate the mean coherency domain and the mean strain (*9*), the reliability factors drop to R_I = 0.035, R_P = 0.065, R_{WP} = 0.063 (Fig. 1). In Table II, the mean particle size and the strain parameters, i.e., the distribution of atoms around their equilibrium positions, are reported. The strain is very weak if compared to cold worked materials for instance, so the line broadening is mainly due to the size effect. The particles are not (001) platelets, as generally observed for brucite-type compounds obtained by precipitation, but the easiest direction of growth appears to be [010].

The hydrogen atoms were located on a difference Fourier map using the neutron diffraction pattern. The vanadium coordinates were fixed at the values they had in the final refinement from the X-ray data. Fermi lengths of D, H, and all of the nonhydrogen atoms were taken from (*10*). The sample was not fully deuterated; therefore the deuterium site occupancy was also refined and corresponds to 74% of deuterium on hydrogen sites; with isotropic temperature factors, this leads to R_I = 0.060; R_P = 0.093; R_{WP} = 0.085 (Fig. 2). Final atomic coordinates and thermal parameters appear in Table III. Selected interatomic distances are listed in Table IV.

Description of the Structure and Structural Correlations

After a discussion in terms of coordination polyhedra and hydrogen bonds,

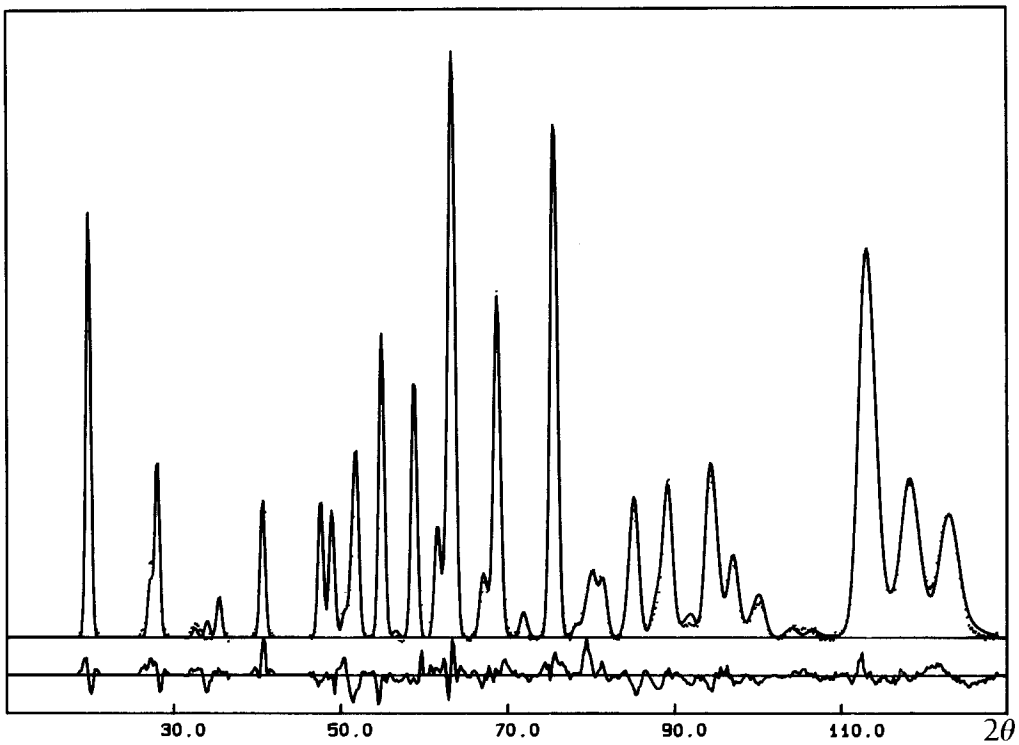

FIG. 2. Observed (...) and calculated (—) neutron powder patterns. The difference appears below at the same scale.

volborthite will be described using two different ways: the layered structure and the pillared one. Finally, other structures which exhibit similar characteristics will be compared to volborthite.

A. Coordination Polyhedra and Hydrogen Bonds

The two types of copper atoms are in octahedral coordination. Cu(2) shows an acceptable (4 + 2)-coordination (4 * Cu–O ≈ 1.9–2.0 Å; 2 * Cu–O ≈ 2.4 Å), i.e., the Jahn–Teller distortion gives rise to the generally observed elongation. On the contrary, the pseudo-tetragonally compressed octahedral coordination of Cu(1) (Table IV) must be considered as dubious in the absence of a precise single crystal structure determination and without the confirmation of spectroscopic data. This anomaly may be, however, tentatively attributed to some kind of competition between the tendency to a ferrodistortive cooperative order (which would have been observed for a long Cu(1)–O(2) distance) expected for such a highly Cu^{2+} concentrated material and the constraints of the topology of the host lattice structure as previously noted by Reinen (*11*). Nevertheless, the crystal chemistry of the structure remains credible.

The short Cu–O(2) distances correspond in fact to bonds between copper and hydroxyl groups (see below). The copper octahedra form layers (Figs. 3 and 4) which will be discussed further.

Vanadium atoms are surrounded tetrahedrally by four oxygen atoms. Three out of the four belong also to the copper octahe-

TABLE III

POSITIONAL AND THERMAL PARAMETERS FROM X-RAY AND NEUTRON REFINEMENTS

Atom	*x/a*	*y/b*	*z/c*	B(Å^2)
Cu(1)	0	0	0	0.69(7)
	0	**0**	**0**	**1.02(13)**
Cu(2)	1/4	1/4	0	1.81(5)
	1/4	**1/4**	**0**	**1.02(13)**
V	0.9959(2)	1/2	0.2516(3)	0.55(5)
	fixed	**fixed**	**fixed**	**fixed**
O(1)	0	1/2	1/2	4.27(31)
	0	**1/2**	**1/2**	**1.50(14)**
O(2)	0.3424(5)	1/2	0.1143(7)	1.55(19)
	0.3428(9)	**1/2**	**0.1095(5)**	**1.50(14)**
O(3)	0.0682(3)	0.2721(6)	0.1846(5)	1.82(12)
	0.0756(7)	**0.2635(12)**	**0.1864(10)**	**1.50(14)**
O(4)	0.1548(5)	1/2	0.8464(7)	2.02(17)
	0.1622(8)	**1/2**	**0.8381(16)**	**1.50(14)**
O(w)	0.3261(5)	1/2	0.4788(7)	4.71(18)
	0.3223(12)	**1/2**	**0.4894(18)**	**1.50(14)**
H(1)	**0.3501(25)**	**1/2**	**0.2376(44)**	**5.7(9)**
H(2)	**0.3536(23)**	**0.3714(33)**	**0.5639(29)**	**5.7(9)**

Note. The values from neutron data appear in bold.

dra, the last, O(1), is shared between the two vanadium tetrahedra of the pyrovanadate groups.

Inbetween the layers and the pyrovanadate groups, the O(w) atoms of the water molecules are inserted and draw a honeycomb sublattice. As predicted by bond valence calculations (*12*), the refinement confirms that O(w) correspond to water molecules H(2)–O(w)–H(2) whereas O(2) linked to three copper atoms correspond to hydroxyl groups –O(2)–H(1).

Hydrogen H(1) gives a hydrogen bond with O(w). Hydrogen H(2) points toward O(3). This justifies that the water molecules are maintained by hydrogen bonding to the layers (Fig. 5). Therefore volborthite can be described by the formulation $Cu_3V_2O_7(OH)_2, 2H_2O$ instead of $Cu_3V_2O_8, 3H_2O$ as claimed before. Infrared analyses confirm the presence of hydroxyl groups together with water molecules.

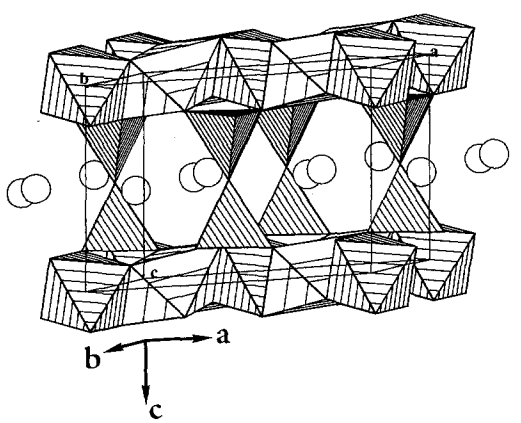

FIG. 3. Perspective view of volborthite. The copper octahedra of the layer are hatched heavily for Cu(1) and slightly for Cu(2), respectively.

TABLE IV

SELECTED INTERATOMIC DISTANCES (Å) AND ANGLES (°) FROM NEUTRON DATA

Cu1 octahedron	
Cu1–O2 = 2 * 1.906(10)	O2–Cu1–O2 = 180.0(7)
Cu1–O3 = 4 * 2.159(7)	O3–Cu1–O3 = 2 * 91.5(6)
	O3–Cu1–O3 = 2 * 180.0(2)
⟨Cu1–O⟩ = 2.075, ($d_{Shannon}$ = 2.110)	O3–Cu1–O3 = 2 * 88.5(6)
	O3–Cu1–O2 = 4 * 91.9(7)
	O3–Cu1–O2 = 4 * 88.1(7)
Cu2 octahedron	
Cu2–O2 = 2 * 1.901(6)	O2–Cu2–O2 = 180.0(6)
Cu2–O4 = 2 * 2.049(15)	O4–Cu2–O4 = 180.0(3)
Cu2–O3 = 2 * 2.380(8)	O3–Cu2–O3 = 180.0(5)
	O4–Cu2–O4 = 2 * 97.0(4)
	O4–Cu2–O4 = 2 * 83.0(8)
⟨Cu2–O⟩ = 2.110, ($d_{Shannon}$ = 2.110)	O3–Cu2–O2 = 2 * 82.0(6)
	O3–Cu2–O2 = 2 * 98.0(5)
	O3–Cu2–O4 = 2 * 87.7(6)
	O3–Cu2–O4 = 2 * 92.3(5)
V^{5+} tetrahedron	
V–O3 = 2 * 1.712(12)	O3–V–O3 = 108.3(7)
V–O4 = 1.746(8)	O4–V–O4 = 2 * 112.3(7)
V–O1 = 1.789(2)	O1–V–O3 = 2 * 107.8(4)
⟨V–O⟩ = 1.739, ($d_{Shannon}$ = 1.735)	O1–V–O1 = 108.2(6)
H1 bonding	
H1–O2 = 0.921(33)	H1–O2–Cu2 = 2 * 114.4(2.6)
H1–Ow = 1.866(34)	H1–O2–Cu1 = 114.4(3.0)
	O2–H1–O5 = 166.1(3.5)
H2 bonding	
H2–Ow–0.969(40)	Ow–H2–O3 = 150.6(1.2)
H2–O3 = 2.051(37)	H2–Ow–H1 = 117.8(2.5)

Note. Vanadium atoms were fixed at the value they had after refinement of the X-ray data. (Ionic radii from Shannon (*19*)).

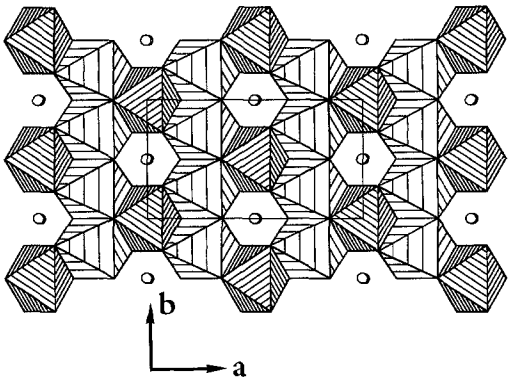

FIG. 4. Projection view along c axis. V atoms are represented as circles. The hatching of octahedra is the same as in the legend to Fig. 3.

pied; MX_6 octahedra share edges with six neighboring octahedra and build up MX_2 planes; such layers are found for instance in $M^{II}(OH)_2$ compounds (M^{II} = Ni, Co, Mg, Fe...) (see, for example, Ref. (*13*)) and in $CuAlO_2$ (*14*) with the delafossite structure. Ordered vacancies can be introduced on the cationic sites of the brucite layer. In $PbSb_2O_6$ (*15*), in thorveitite-like compounds: $Cd_2V_2O_7$ (*16*), $Mg_2As_2O_7$ (*17*)... the layers, in which one-third of the octahedral sites are vacant, have $\square M_2X_6$ formulation (Fig. 6b) (M = Sb, Cd, Mg).

In volborthite layers, copper atoms occupy three-fourths of the octahedral sites,

B. Brucite-Type Layers

As noted in section A, copper octahedra build up (001) layers that we shall call defect brucite-like layers (thereafter noted DBL). Indeed, in the brucite-type layers (Fig. 6a) all the octahedral sites are occu-

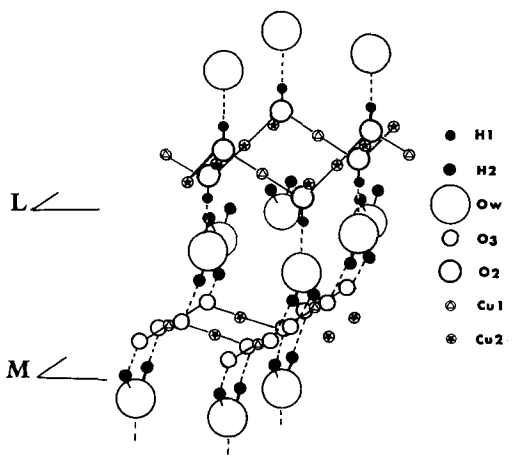

FIG. 5. A simplified view of hydrogen bonds. (L) and (M) represent $\square Cu_3O_8$ layers and only anions which lead to the formation of hydrogen bonds are drawn. (L) evidences hydrogen bonds with H(1), with the formation of hydroxyl groups –O(2)–H(1), (M) hydrogen bonds with H(2), H(2) pointing toward O(3). Inbetween the layers appear water molecules H(2)–O(w)–H(2), H(1) forming a hydrogen bond with O(w).

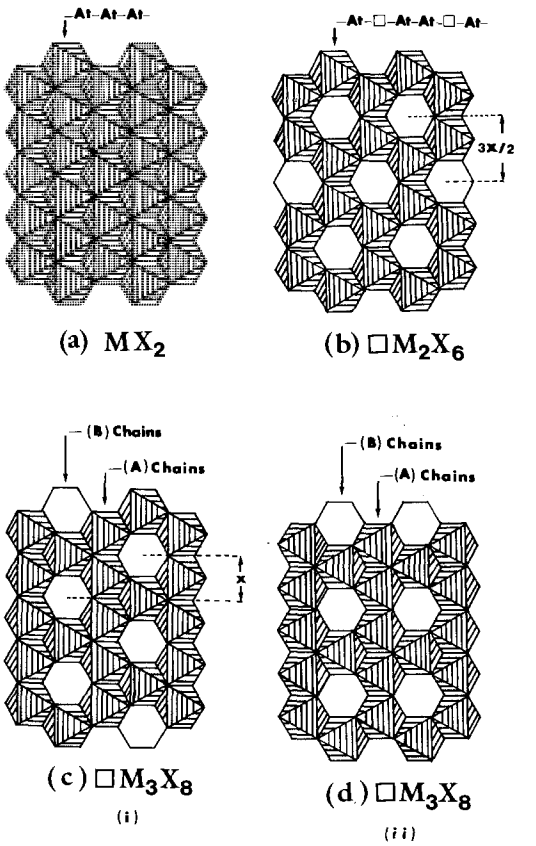

FIG. 6. Brucite-like layers: (a) MX_2, brucite layer; (b) $\square M_2X_6$; (c) (d) $\square M_3X_8$, defect brucite layers (DBL).

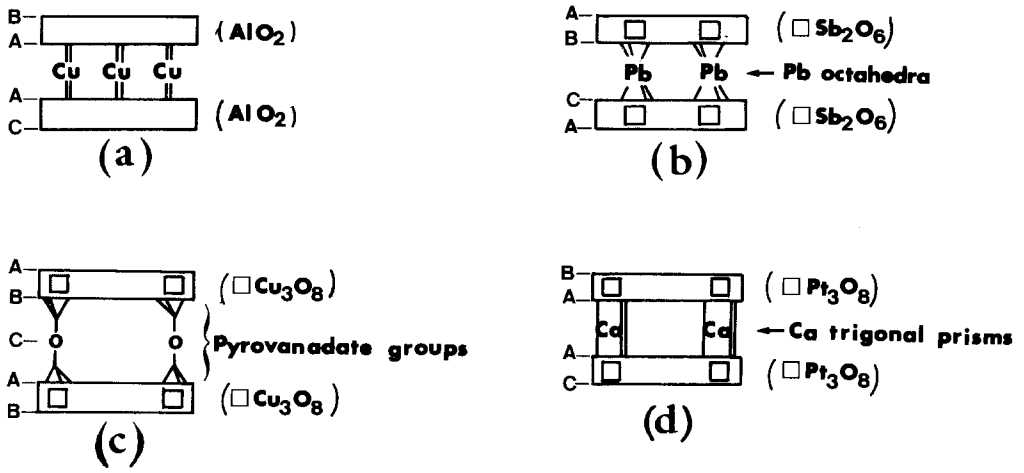

FIG. 7. Pillared structures built up from defect brucite layers (DBL). (□ corresponds to a vacancy). (a) $CuAlO_2$; (b) $PbSb_2O_6$; (c) $Cu_3V_2O_7(OH)_2, 2H_2O$; (d) $Ca_2Pt_3O_8$.

as in the $Ca_2Pt_3O_8$ structure (*18*); this leads to the formulation (i) $\square M_3X_8$, where the vacancies are hexagonally ordered (Fig. 6c). This same formulation is encountered in another kind of layer where the isolated vacancies are orthorhombically ordered (Fig. 6d, ii). This DBL is found in $A_2Mn_3O_8$ (A = Co, Zn, Cu, Mn, Ca, Cd...), $A_2Mo_3O_8$ (A = Co, Zn, Mn, Fe...), and isostructural nolanite compounds (Refs. in (*18*)). In terms of plane nets of copper atoms, this means that the Schläfli symbol (*20*) is [6.3.6.3] and $[(3^2.6^2)^2, 6.3.6.3]$ for (i) and (ii), respectively.

A more accurate description of the volborthite layer can be given considering that the layer is composed of two kinds of rutile-like chains extended in the b direction. Filled chains of Cu(2) atoms ..–Cu(2)–Cu(2)–Cu(2)–..: (type A) alternate with half-filled chains of Cu(1) atoms ..–Cu(1)–□–Cu(1)–□–..: (type B). Two consecutive (A) chains, separated by a (B) one, are shifted by the distance x (= $b/2$ for volborthite) (Fig. 4) at variance to layers of (ii) formulation where no shift is observed. Using such a description, the $\square M_2X_6$ layer is composed of ..–At–□–At–At–□–At–.. chains successively shifted by the distance $3x/2$ (Fig. 6b).

C. Pillared Structure

Among the different compounds named before, just a few of them exhibit pillars in the interlayer region, depending on the composition of the layers.

A pillared structure with an MX_2 composition is illustrated by the delafossite-type compound $CuAlO_2$. In the interlayer space, the Cu atoms are linearly coordinated by two oxygen atoms belonging to the AlO_2 layers. (Fig. 7a). All the oxygen atoms of a layer are linked to copper. The bridging units, perpendicular to the layers, correspond to a close-packing ..BBAACC...

For DBL layers, the best place for the location of linking units is above and below the windows of the Kagomé layers. Among the $\square M_2X_6$-layered compounds noted before, only $PbSb_2O_6$ (*15*) exhibits a pillared structure. Figure 7b illustrates the Pb atoms which use six oxygens of the layers to ensure an octahedral pillar. The Pb octahedra are located above and below two-thirds of the empty octahedral interstices of the $\square Sb_2O_6$ layers. This leads to the formation

of a hexagonal array of close-packed oxygen atoms (..ABC..).

$Cu_3V_2O_7(OH)_2$, $2H_2O$ and $Ca_2Pt_3O_8$ are examples of pillared structures built up from $\square M_3X_8$ (i) sheets. In $Ca_2Pt_3O_8$ the $\square Pt_3O_8$ sheets are connected by Ca atoms in trigonal prismatic coordination; (Fig. 7d). It gives rise to –AABBCC– arrangement.

In isostructural nolanite compounds, only $A_2Mn_3O_8$ compounds (A = Mn, Ca, Cd) adopt a pillared structure built up from (ii) sheets with A in trigonal prismatic sites. It leads to ...AABBCC... arrangement identical to that of $Ca_2Pt_3O_8$.

In the case of volborthite, the bridging units are pyrovanadate groups. They introduce new oxygen planes with vacant anionic sites (Fig. 7c), increase the intersheet distances, and allow water molecules to be located in the interlayer region. This leads to the formation of a pseudo hexagonal close-packed arrangement of oxygen planes (..ABC..). This provides a good example of the influence of the nature of the bridging unit, located above and below the empty octahedra, for the control of the type of close-packed arrangement.

Conclusion

This structural study shows that volborthite is a hydrated basic salt with the formulation $Cu_3V_2O_7(OH)_2$, $2H_2O$. It exhibits an interesting structural topology with layers, pillars, and hydrogen bonding networks. The thermal behavior of this hydrated phase and the structural phase transition which occurs in the anhydrous compound will be described in a future paper.

Acknowledgments

The authors are very grateful to Professor M. Leblanc (Université du Maine) for fruitful discussions and to Drs. J. Rodriguez and J. Pannetier (ILL Grenoble) for their helping during the neutron diffraction experiment.

References

1. C. Guillemin, *Bull. Soc. Fr. Mineral. Cristallogr.* **79,** 238 (1956).
2. E. S. Leonardsen and O. V. Petersen, *Amer. Mineral.* **59,** 372 (1974).
3. N. Strupler, *Ann. Chim.* **10,** 345 (1965).
4. H. F. McMurdie, M. C. Morris, E. H. Evans, B. Paretzkin, W. Wong-Ng, and C. R. Hubbard, *Powder Diffraction* **1,** 40 (1986).
5. A. Le Bail, H. Duroy, and J. L. Fourquet, *Mater. Res. Bull.* **23,** 447 (1988).
6. G. M. Sheldrick, "SHELX76, Program for Crystal Structure Determination," Univ. of Cambridge, England (1976).
7. "International Tables for X-Ray Crystallography," Vol. IV, Kynoch Press, Birmingham. (Present distributor: Reidel, Dordrecht.)
8. T. Suzuki, *Acta Crystallogr.* **13,** 279 (1960).
9. C. Lartigue, A. Le Bail, and A. Percheron-Guegan, *J. Less-Common Met.* **129,** 65 (1987).
10. V. F. Sears, "Thermal Neutron Scattering Lengths and Cross Sections for Condensed Matter Research," Internal Report AECL 8490, Chalk River Lab. (1984).
11. D. Reinen, *J. Solid State Chem.* **27,** 71, (1979).
12. I. D. Brown, "The Bond Valence Method; An Empirical Approach to Chemical Structure and Bonding in "Structure and Bonding in Crystals" (O'Keeffe and Navrotsky, Eds.), Vol. 2, p. 1, Academic Press, San Diego (1981), and all references therein.
13. R. W. G. Wyckoff, "Crystal Structures," Vol. 1, Interscience, New York (1960).
14. T. Ishiguro, N. Ishizawa, N. Mizutani, and M. Kato, *J. Solid State Chem.* **41,** 132 (1982).
15. R. J. Hill, *J. Solid State Chem.* **71,** 12 (1987).
16. P. K. L. Au and C. Calvo, *Canad. J. Chem.* **45,** 2297 (1967).
17. C. Calvo and K. Neelakantan, *Canad. J. Chem.* **48,** 890 (1970).
18. X. Turrillas, C. Laviron, H. Vincent, J. Pannetier, and J. C. Joubert, *J. Solid State Chem.* **67,** 297 (1987).
19. R. D. Shannon, *Acta Crystallogr. A* **32,** 751 (1976).
20. M. O'Keeffe and B. G. Hyde, *Philos. Trans. R. Soc. London, Sec. A* **295,** 553 (1980).